

Supporting Information:

Insight into trifluoromethylation - experimental electron density for Togni reagent 1.

Ruimin Wang, Irmgard Kalf and Ulli Englert

September 25, 2018

List of Tables

S1	Crystal data and refinement results for 1	2
S2	Resolution & completeness statistics (cumulative and Friedel pairs averaged)	3
S3	R-value statistics (IAM) as a function of resolution (in resolution shell)	3
S4	Bond distances (Å) for 1	5
S5	Bond angles (°) for 1	5
S6	Monopole and dipole populations, radial parameters and net atomic charges.	7
S7	Topological properties of (3, -1) critical points for the most relevant intermolecular interactions and chemical bonds ; d_1 (d_2) is the distance from the first (second) atom to the (3, -1) critical point, $R_{ij} = d_1 + d_2$, ρ is the electron density, $\nabla^2\rho$ is the Laplacian of the electron density.	8
S8	Topological properties of (3, -1) critical points for secondary intermolecular interactions ; d_1 (d_2) is the distance from the first (second) atom to the (3, -1) critical point, $R_{ij} = d_1 + d_2$, ρ is the electron density, $\nabla^2\rho$ is the Laplacian of the electron density.	9

List of Figures

S1	MM refinement results for 1	4
S2	Scatterplot F_{obs}^2/F_{calc}^2 vs $\sin\theta/\lambda$ for X-ray refinement result (MM) for 1	5
S3	Scatterplot F_{obs}^2 vs F_{calc}^2 for X-ray refinement result for 1	6
S4	Trajectory plots showing $ \nabla\rho $; bond paths are drawn as black lines, bond critical points as blue solid circles, and ring critical points as green solid circles.	8
S5	Laplacian of the experimental electron density ($\nabla^2\rho$); isosurface= $-3 e\cdot\text{Å}^{-5}$	9
S6	Fractal dimension plots [3, 4] vs residual electron density.	10
S7	Normal probability plots [3, 4] vs residual electron density.	10

1 Crystal data and refinement results for 1.

Table S1: Crystal data and refinement results for 1.

Compound	1	
Moiety formula	C ₁₀ H ₁₀ F ₃ IO	
Formula weight ($g \cdot mol^{-1}$)	330.08	
Crystal description	colorless, block	
Crystal size (mm)	0.36 x 0.19 x 0.09	
Crystal system	monoclinic	
Space group	$P2_1/n$	
a (Å)	9.1507(5)	
b (Å)	9.0836(5)	
c (Å)	13.3668(7)	
β (°)	93.2446(16)	
V (Å ³)	1109.28(10)	
Z	4	
μ (mm ⁻¹)	2.899	
$\sin \theta_{max}/\lambda$	1.1 Å ⁻¹	
Total/unique reflections	151509/12366	
R_{int}	0.0530	

Refinement	IAM	MM
$R_1(I > 2\sigma(I))$	0.0221	0.019
$wR_2(F^2)$	0.0552	0.050
GOF	1.084	1.056
No. of parameters	138	543
$\Delta\rho_{max}/\Delta\rho_{min}(e \text{ Å}^{-3})$	1.593/-0.771	0.895/-0.889
CCDC	1862413	1862414

2 Data collection details

Temperature (K)	100
Radiation (Å)	MoK α 0.71073
θ Min–Max (°)	2.6–55.1
Dataset	-20: 20 ; -20: 20 ; -30: 30
Tot., Uniq. Data, R(int)	159334, 14149, 0.0538

Table S2: Resolution & completeness statistics (cumulative and Friedel pairs averaged)

θ	$\sin\theta/\lambda$	Complete	Expected	Measured	Missing
20.82	0.500	1.000	1157	1157	0
23.01	0.550	1.000	1542	1542	0
25.24	0.600	1.000	2000	2000	0
27.51	0.650	1.000	2559	2559	0
29.84	0.700	1.000	3189	3189	0
32.21	0.750	1.000	3927	3927	0
34.65	0.800	1.000	4762	4762	0
37.17	0.850	1.000	5718	5718	0
39.77	0.900	1.000	6772	6772	0
42.47	0.950	1.000	7973	7973	0
45.29	1.000	1.000	9298	9298	0
48.27	1.050	1.000	10748	10748	0
51.43	1.100	1.000	12362	12362	0
54.82	1.150	0.998	14123	14097	26
55.11	1.154	0.992	14262	14149	113

3 Structure refinement

Table S3: R-value statistics (IAM) as a function of resolution (in resolution shell)

θ	$\sin\theta/\lambda$	#	R_1	$wR2$	S	R_s	$av(I/SigW)$	$av(I)$	$av(SigW)$
12.38	0.302	258	0.027	0.075	2.370	0.019	30.81	7684.49	232.92
15.68	0.380	249	0.017	0.054	1.665	0.017	29.95	4296.55	126.04
18.02	0.435	252	0.017	0.050	1.446	0.018	27.60	3100.26	93.40
19.90	0.479	262	0.017	0.053	1.441	0.020	25.31	2190.16	68.69
21.51	0.516	261	0.016	0.047	1.263	0.020	25.44	2179.71	69.52
22.94	0.548	245	0.017	0.049	1.309	0.019	24.59	1716.46	54.39
24.22	0.577	262	0.016	0.047	1.243	0.019	24.57	1442.65	45.38
25.40	0.603	246	0.020	0.054	1.422	0.017	24.45	1234.09	38.29
26.49	0.628	264	0.019	0.050	1.331	0.017	24.27	986.24	30.81
27.52	0.650	261	0.019	0.049	1.278	0.017	23.71	896.15	28.32
28.49	0.671	253	0.017	0.047	1.224	0.017	23.50	798.82	25.47
29.41	0.691	250	0.016	0.043	1.106	0.018	23.68	770.07	24.99
30.28	0.709	247	0.017	0.043	1.059	0.019	22.42	732.15	24.25
31.12	0.727	273	0.015	0.038	0.883	0.021	20.63	626.76	21.96
31.93	0.744	247	0.019	0.045	1.000	0.024	19.61	572.09	21.24
32.71	0.760	254	0.020	0.049	1.112	0.025	20.58	580.90	21.75
33.46	0.776	250	0.023	0.052	1.088	0.026	18.46	445.36	17.63
34.20	0.791	269	0.021	0.051	1.052	0.027	17.98	417.19	16.58
34.91	0.805	265	0.020	0.047	0.957	0.028	17.84	398.56	16.40
55.11	1.154	9281	0.032	0.070	0.910	0.059	9.74	156.91	11.22

$$R_\sigma = \sum(\sigma(I))/\sum(I) = 0.0255$$

4 MM Refinement

A more appropriate model for the electron density is based on *atom-centered multipolar functions* [1].

$$\begin{aligned}\rho_{pseudoat.}(r) &= \rho_{core}(r) + P_v \kappa^3 \rho_{valance}(\kappa r) + \rho_{def}(\kappa' r) \\ \rho_{def}(\kappa' r) &= \sum_{l=0}^{l_{max}} \kappa'^3 R_l(\kappa' r) \sum_{m=0}^l P_{lm\pm} d_{lm\pm}(\theta, \phi)\end{aligned}$$

After convergence of this multipole model (MM), the deformation density defined by $\rho_{MM} - \rho_{IAM}$ provides a more detailed picture of bonding effects. As expected, the deformation densities in both residues reflect the effects of covalent bonding more clearly and with less noise than a residual density map based on the IAM.

Refinement was conducted with all intensity data, $\sin\theta/\lambda \leq 1.1$. The final Multipole refinements on F^2 comprised multipoles up to hexadecapoles for non-H atoms and up to bond-directed dipoles for the H atoms. In the MM, C-H distances were constrained to 1.09 Å. κ' of I was fixed to 1.5, and contraction parameters for the remaining non-H atoms were refined freely in a step-wise approach.

```
Residuals after cycle 7
R{ F } = 0.0260          Rw{ F } = 0.0269
R{F^2} = 0.0277          Rw{F^2} = 0.0506
GOFw = 1.0539          GOF = 1.3130  Nref/Nv = 23.3321
-----
Mean(Shift/su) = 0.740530E-06
Max(Shift/su) = 0.527032E-05 for variable  F(2)/M1
-----
Atom-Group(s) (net charge)
1 (-0.00050)
-----
After cycle 7 convergence criterion was met
Proceed to last cycle to finalise outputs
-----
Number of data = 12366
Rejected based on OBS = 0
Rejected based on SIGOBS = 0
Rejected based on SINTHL = 0
Total number of rejections = 0
Included in the refinement = 12366
-----
Residuals after final cycle
R{ F } = 0.0260          Rw{ F } = 0.0269
R{F^2} = 0.0277          Rw{F^2} = 0.0506
GOFw = 1.0539          GOF = 1.3130  Nref/Nv = 23.3321
-----
```

1

Figure S1: MM refinement results for **1**.

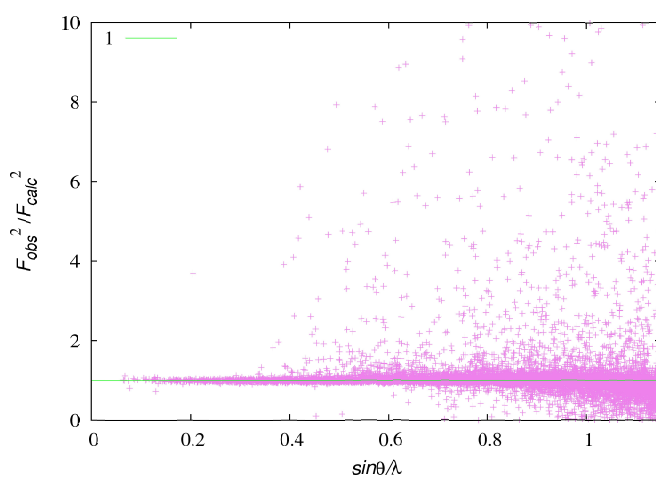
Table S4: Bond distances (Å) for **1**.

O1...I1 ⁱ	2.9826(9)	I1—C10	2.1119(7)
I1—O1	2.1241(9)	I1—C1	2.2753(7)
F1—C1	1.3492(17)	F2—C1	1.3445(17)
F3—C1	1.3498(17)	O1—C2	1.4124(12)
C2—C4	1.5236(13)	C2—C3	1.5425(15)
C2—C5	1.5269(10)	C5—C10	1.3862(10)
C5—C6	1.3986(11)	C6—C7	1.3935(13)
C7—C8	1.3898(15)	C8—C9	1.3956(12)
C9—C10	1.3908(9)	O1...O1 ⁱ	2.795(2)

$$i = 1 - x, 1 - y, 1 - z$$

Table S5: Bond angles (°) for **1**.

O1 — C2 — C4	107.28(8)
O1 — C2 — C5	107.99(7)
C4 — C2 — C5	111.61(8)
C2 — C5 — C6	123.48(7)
C2 — C5 — C10	119.01(6)
C6 — C5 — C10	117.48(7)
C5 — C6 — C7	120.80(9)
C6 — C7 — C8	120.09(9)
C7 — C8 — C9	120.40(7)
C8 — C9 — C10	118.00(8)
C5 — C10 — C9	123.23(7)

**Figure S2:** Scatterplot F_{obs}^2/F_{calc}^2 vs $\sin\theta/\lambda$ for X-ray refinement result (MM) for **1**.

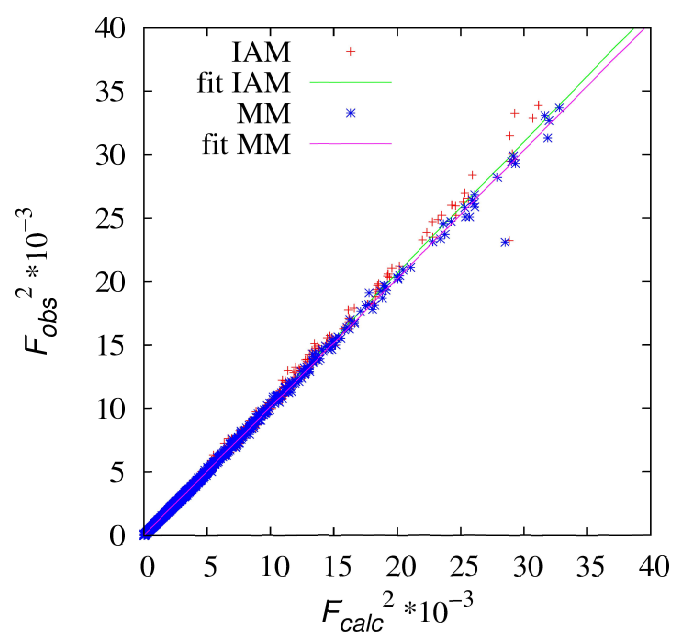


Figure S3: Scatterplot F_{obs}^2 vs F_{calc}^2 for X-ray refinement result for **1**.

Contraction parameters and multipole population coefficients

Table S6: Monopole and dipole populations, radial parameters and net atomic charges.

Atom	κ	κ'	Net charge	atom	P_v	P_{00}	P_{11}	P_{1-1}	P_{10}
I(1)	1.203(12)	1.500	+0.96(17)	I(1)	6.04(17)	0.00(0)	-0.03(3)	-0.03(2)	-0.11(2)
F(1)	0.971(5)	1.03(7)	-0.18(8)	F(1)	7.18(8)	0.00(0)	0.11(4)	-0.13(4)	0.05(3)
F(2)	0.971(5)	1.03(7)	-0.25(8)	F(2)	7.25(8)	0.00(0)	0.03(4)	0.00(4)	0.01(3)
F(3)	0.971(5)	1.03(7)	-0.29(8)	F(3)	7.29(8)	0.00(0)	0.06(4)	-0.09(4)	0.01(3)
O(1)	0.973(7)	1.18(11)	-0.36(6)	O(1)	6.36(6)	0.00(0)	-0.01(3)	-0.04(2)	-0.08(2)
C(1)	0.923(17)	0.83(4)	-0.37(10)	C(1)	4.37(10)	0.00(0)	-0.13(5)	-0.13(5)	-0.08(5)
C(2)	0.93(2)	0.71(3)	-0.58(16)	C(2)	4.58(16)	0.00(0)	-0.21(10)	0.01(10)	0.02(9)
C(3)	0.926(16)	0.89(5)	-1.04(17)	C(3)	5.04(17)	0.00(0)	-0.01(6)	-0.15(7)	0.22(6)
C(4)	0.926(16)	0.89(5)	-0.31(17)	C(4)	4.31(17)	0.00(0)	0.08(6)	0.31(7)	0.04(6)
C(5)	0.956(6)	0.752(18)	+0.6(3)	C(5)	3.4(3)	0.00(0)	0.23(10)	0.14(13)	0.33(13)
C(6)	0.956(6)	0.752(18)	-0.1(3)	C(6)	4.1(3)	0.00(0)	0.00(10)	-0.23(13)	-0.06(12)
C(7)	0.956(6)	0.752(18)	-0.4(3)	C(7)	4.4(3)	0.00(0)	0.07(11)	0.18(14)	-0.08(13)
C(8)	0.956(6)	0.752(18)	+0.2(3)	C(8)	3.8(3)	0.00(0)	-0.08(10)	0.07(15)	0.19(12)
C(9)	0.956(6)	0.752(18)	-0.2(2)	C(9)	4.2(2)	0.00(0)	0.00(9)	-0.14(12)	-0.05(11)
C(10)	0.956(6)	0.752(18)	-0.3(2)	C(10)	4.3(2)	0.00(0)	0.06(9)	-0.04(11)	-0.07(11)
H(3A)	1.200	1.200	+0.27(7)	H(3A)	0.73(7)	0.00(0)	0.00(0)	0.00(0)	0.07(5)
H(3B)	1.200	1.200	+0.14(8)	H(3B)	0.86(8)	0.00(0)	0.00(0)	0.00(0)	0.12(5)
H(3C)	1.200	1.200	+0.09(8)	H(3C)	0.91(8)	0.00(0)	0.00(0)	0.00(0)	0.09(5)
H(4A)	1.200	1.200	+0.51(8)	H(4A)	0.49(8)	0.00(0)	0.00(0)	0.00(0)	0.02(6)
H(4B)	1.200	1.200	+0.30(9)	H(4B)	0.70(9)	0.00(0)	0.00(0)	0.00(0)	0.16(6)
H(4C)	1.200	1.200	-0.02(8)	H(4C)	1.02(8)	0.00(0)	0.00(0)	0.00(0)	0.22(5)
H(6)	1.200	1.200	+0.29(8)	H(6)	0.71(8)	0.00(0)	0.00(0)	0.00(0)	0.18(4)
H(7)	1.200	1.200	+0.25(8)	H(7)	0.75(8)	0.00(0)	0.00(0)	0.00(0)	0.23(5)
H(8)	1.200	1.200	+0.41(8)	H(8)	0.59(8)	0.00(0)	0.00(0)	0.00(0)	0.23(4)
H(9)	1.200	1.200	+0.33(7)	H(9)	0.67(7)	0.00(0)	0.00(0)	0.00(0)	0.14(4)

5 Topological analysis (AIM)

5.1 Bond critical points and zero flux surfaces of electron density

The electron density modeled by the multipole refinement, $\rho(r)$ was analysed using Bader's quantum theory of atoms in molecules, QTAIM [2], and the critical points of the electron density were identified. Intermolecular interactions show up in the trajectory plots in S4. They depict the derivative of the electron density.

$$\vec{\nabla}\rho = \frac{\partial\rho}{\partial x}\vec{i} + \frac{\partial\rho}{\partial y}\vec{j} + \frac{\partial\rho}{\partial z}\vec{k}$$

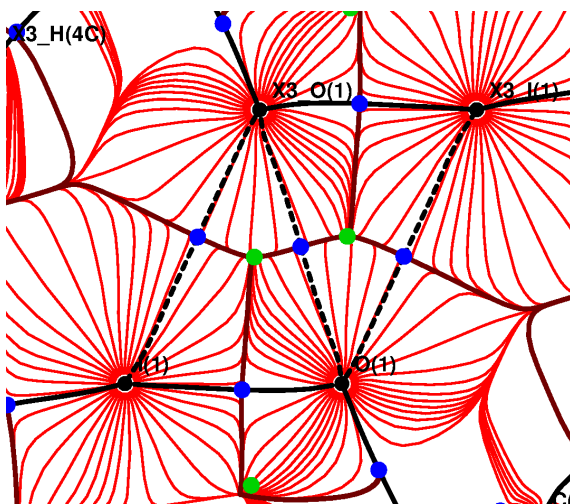


Figure S4: Trajectory plots showing $|\nabla\rho|$; bond paths are drawn as black lines, bond critical points as blue solid circles, and ring critical points as green solid circles.

Saddle points with $\nabla\rho(r) = 0$, so-called bond critical points (*bcp*), are shown as blue circles. Numerical values for *bcp* geometries, their electron densities and derived properties have been compiled in table S8.

Table S7: Topological properties of (3, -1) critical points for the most relevant intermolecular interactions and chemical bonds; d_1 (d_2) is the distance from the first (second) atom to the (3, -1) critical point, $R_{ij} = d_1 + d_2$, ρ is the electron density, $\nabla^2\rho$ is the Laplacian of the electron density.

Bond	dist.(Å)	R_{ij} (Å)	d_1 (Å)	d_2 (Å)	$\rho(e\cdot\text{Å}^{-3})$	$\nabla^2\rho(e\cdot\text{Å}^{-5})$
I(1)⋯O(1) ⁱ	2.9826(9)	2.9824	1.5992	1.3832	0.102(2)	1.307(3)
O(1)⋯O(1) ⁱ	2.795(2)	2.7933	1.3967	1.3967	0.095(3)	1.332(6)
I(1)—O(1)	2.1241(9)	2.1270	1.1470	0.9800	0.64(2)	7.91(6)
I(1)—C(1)	2.2753(7)	2.2761	1.1721	1.1039	0.78(2)	1.72(6)
I(1)—C(10)	2.1119(7)	2.1409	1.1690	0.9719	0.71(2)	2.66(6)
F(1)—C(1)	1.3492 (17)	1.3481	0.9222	0.4259	1.87(5)	-6.7(3)
F(2)—C(1)	1.3445(17)	1.3462	0.9171	0.4291	1.83(5)	-5.6(3)
F(3)—C(1)	1.3498(17)	1.3625	0.9260	0.4366	1.84(5)	-6.8(3)
O(1)—C(2)	1.4124(12)	1.4134	0.9469	0.4665	1.96(4)	-18.0(2)
C(2)—C(3)	1.5425(15)	1.5430	0.6755	0.8676	1.54(4)	-10.65(7)
C(2)—C(4)	1.5236(13)	1.5321	1.0752	0.4569	1.72(7)	-12.0(4)
C(2)—C(5)	1.5269(10)	1.5290	0.8446	0.6845	1.67(4)	-13.74(9)
C(5)—C(6)	1.3986(11)	1.3994	0.6013	0.7981	2.17(4)	-24.1(2)
C(5)—C(10)	1.3863(10)	1.3867	0.6531	0.7336	2.23(4)	-22.3(2)
C(6)—C(7)	1.3935(13)	1.3934	0.6739	0.7195	2.26(4)	-22.8(2)
C(7)—C(8)	1.3898(15)	1.3901	0.7672	0.6229	2.25(4)	-25.0(2)
C(8)—C(9)	1.3956(12)	1.3969	0.6748	0.7221	2.15(4)	-22.5(2)
C(9)—C(10)	1.3908(9)	1.3910	0.6339	0.7571	2.08(4)	-20.2(2)

Table S8: Topological properties of (3, -1) critical points for secondary intermolecular interactions ; d_1 (d_2) is the distance from the first (second) atom to the (3, -1) critical point, $R_{ij} = d_1 + d_2$, ρ is the electron density, $\nabla^2\rho$ is the Laplacian of the electron density.

Bond	dist.(Å)	R_{ij} (Å)	d_1 (Å)	d_2 (Å)	$\rho(e\cdot\text{Å}^{-3})$	$\nabla^2\rho(e\cdot\text{Å}^{-5})$
F(3)···H(8) ⁱⁱ	2.55	2.6207	1.5705	1.0503	0.02(2)	0.451(3)
C(8)···H(3B) ⁱⁱⁱ	2.87	2.9028	1.8833	1.0194	0.047(6)	0.304(2)
H(3A)···F(2) ^{iv}	2.63	2.6288	1.1133	1.5155	0.04(2)	0.507(5)
H(4C)···F(1) ⁱ	2.70	3.0380	1.3153	1.7227	0.012(5)	0.199(3)

$i = 1-x, 1-y, 1-z$; $ii = 1-x, 1-y, -z$; $iii = 0.5-x, -0.5+y, 0.5-z$; $iv = -0.5+x, 0.5-y, 0.5+z$

5.2 The Laplacian of the electron density

The Laplacian of the electron density represents a sensitive tool for establishing the closed-shell or shared character of an interaction and for visualizing local charge accumulations and depletions.

$$\nabla^2\rho = \frac{\partial^2\rho}{\partial x^2} + \frac{\partial^2\rho}{\partial y^2} + \frac{\partial^2\rho}{\partial z^2}$$

Electron densities in the *bcps* of all but the strongest secondary interactions are an order of magnitude lower than those in covalent bonds. The electronic properties of the bonds connecting I1 to its neighbours C1, C10, O1 are more reminiscent of coordinative bonds than of covalent bonds. This similarity with coordinative bonds also holds true for the geometry of the bond paths.

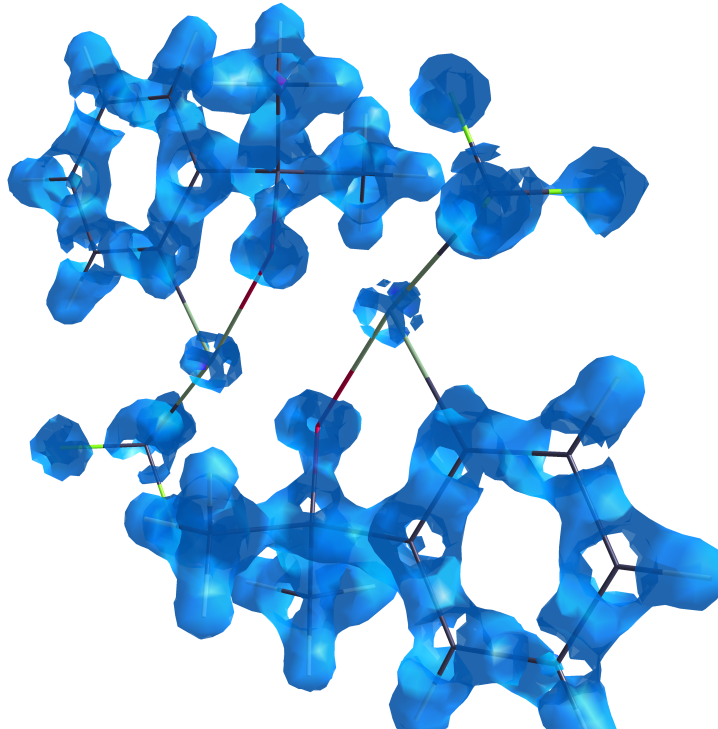


Figure S5: Laplacian of the experimental electron density ($\nabla^2\rho$); isosurface= $-3 e\cdot\text{Å}^{-5}$.

6 Residual electron density distribution

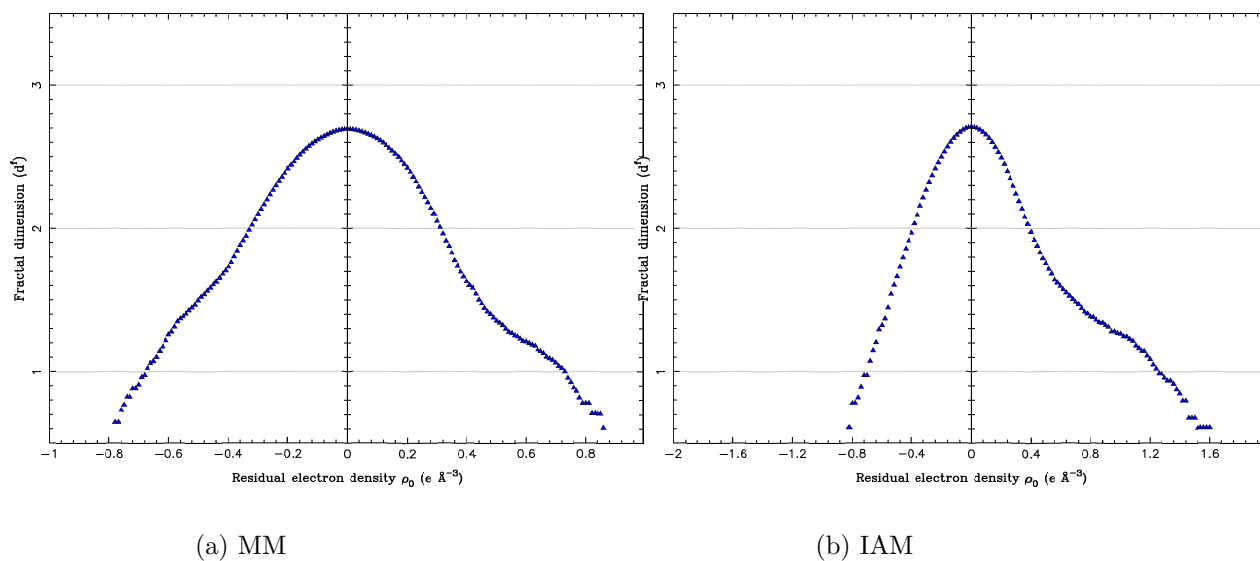


Figure S6: Fractal dimension plots [3, 4] vs residual electron density.

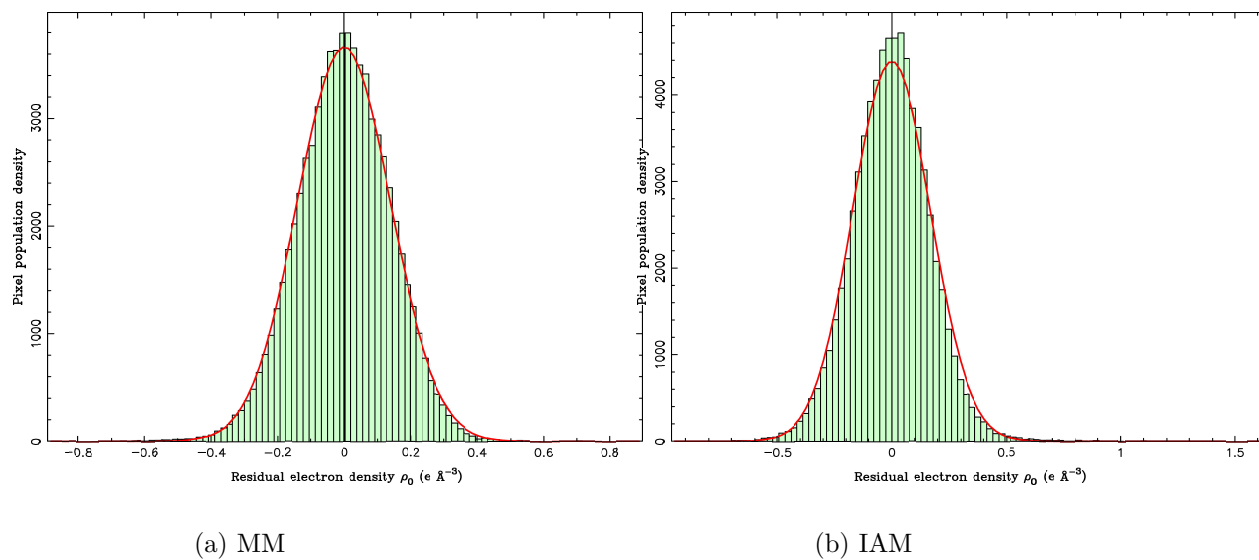


Figure S7: Normal probability plots [3, 4] vs residual electron density.

References

- [1] N. K. Hansen and P. Coppens. Testing aspherical atom refinements on small-molecule data sets. *Acta Crystallogr.*, **1978**, *A34*, 909–921.
- [2] R. F. W. Bader. *Atoms in Molecules - A Quantum Theory*. Oxford University Press: Oxford, U.K., 1990.

- [3] K. Meindl and J. Henn. Foundations of Residual-Density Analysis. *Acta Crystallogr.* **2008**, *A64*, 404–418.
- [4] A. Volkov, P. Macchi, L. J. Farrugia, C. Gatti, P. Mallinson, T. Richter, and T. Koritsanszky. *XD2016 - A Computer Program Package for Multipole Refinement, Topological Analysis of Charge Densities and Evaluation of Intermolecular Energies from Experimental and Theoretical Structure Factors.* **2016**.